Article:

1   **Centrifuge modelling of piled foundations in swelling clays**

2

3   Author 1

4   •   T.A.V. Gaspar, PhD (Pretoria) – corresponding author
5   •   Department of Civil Engineering, University of Pretoria, Pretoria, South Africa
6   •   https://orcid.org/0000-0002-3746-2714
7   •   Present address:
8   o   Department of Civil and Structural Engineering, University of Sheffield, United
9   Kingdom
10   o   Sheffield, S1 3JD
11   Author 2

12   •   S.W. Jacobsz, PhD (Cantab)
13   •   Department of Civil Engineering, University of Pretoria, Pretoria, South Africa
14   •   https://orcid.org/ 0000-0002-7439-2276

15   Author 3

16   •   G. Smit, PhD (Southampton)
17   •   Department of Civil Engineering, University of Pretoria, Pretoria, South Africa

18   Author 4

19   •   A.S. Osman, PhD (Cantab)
20   •   Department of Engineering, Durham University, United Kingdom
21   •   https://orcid.org/0000-0002-5119-8841

22

23   Full contact details of corresponding author

24   •   Email address 1: t.a.gaspar@sheffield.ac.uk
25   •   Email address 2: tav.gaspar@gmail.com
26   •   Mobile: +447488560650

27

28

29

30

31

32

33

34 **Abstract**

35 A study aimed towards assessing the variation in shaft capacity of piled foundations in swelling

36 clays is presented. At the clay's in-situ water content, the results of pull-out tests on short

37 length piles revealed no dependency of shaft capacity on overburden stress. Conversely, after

38 achieving a targeted value of swell, a strong dependency on overburden stress was observed.

39 In upper portions of the profile where swell can occur relatively freely, swell-induced softening

40 results in a reduction in pile shaft capacity. However, at greater depths where swell is largely

41 suppressed, so too are the effects of swell-induced softening. For this reason, shaft capacity

42 at depth was found to remain relatively constant before and after swell. The results of an

43 instrumented pile test revealed an overriding dependency of lateral induced swell pressure on

44 the magnitude of heave which has occurred. Irrespective of the level of overburden stress,

45 lateral pressures against the pile were found to increase at early stages of the swelling

46 process, but then reduce as swell continued and softening began to occur. Such a result

47 highlights the importance of specifying the level of swell at which shaft capacity should be

48 assessed if a conservative design is to be obtained.

49

50 **Keywords: expansive soils; centrifuge modelling; piles and piling; partial saturation**

51

52 *List of notations*

53 e void ratio

54 N centrifuge model scaling factor

55 $\bar{p}$ net-mean stress

56 s suction

57 S_r degree of saturation

58

59

60 ***Introduction***

61 The severe economic implications associated with construction on expansive clays (Jones

62 and Holtz 1973; Jones and Jefferson 2012) have necessitated the implementation of

63 specialised foundation solutions. Measures taken to mitigate the effects of this problem soil

64 can broadly be divided into three categories, namely soil treatment or replacement,

65 construction directly on the expansive profile and, isolation of the superstructure from the

66 expansive profile.

67

68 Removal and replacement is generally a feasible approach if the depth of expansive material

69 is shallow (approximately 2 m deep) and when suitable inert material is readily available

70 (Byrne *et al.* 2019). Alternatively, the soil can be 'treated' by pre-wetting the profile such that

71 swell occurs before construction, thus limiting structural distress. Drawbacks of this approach

72 include the time taken for the soil to reach an equilibrium moisture content, and the uncertainty

73 of future changes in moisture throughout the lifetime of the structure (Byrne *et al.* 2019).

74 Arguably the most common approach for foundation design on swelling clays is to utilise a

75 stiffened raft foundation (Byrne *et al.* 2019; Charlie *et al.* 1985; Li *et al.* 2014; Pellissier, 1997).

76 The rationale behind such a foundation type is to prevent differential movements across the

77 foundation, thereby limiting structural distress. Isolation of the superstructure from the

78 underlying expansive soil is the most expensive of the three approaches mentioned. The

79 approach typically involves the use of piled foundations extending either to bedrock where

80 they can be socketed, or to a stable soil horizon where the foundation can be anchored using,

81 for example, enlarged base piles (Byrne *et al.* 2019). These piles are then used to support a

82 suspended foundation which is completely isolated from the underlying soil. The gap provided

83 between the suspended foundation and the ground level provides space for the soil to swell

84 into, without affecting the superstructure.

85 Piles used in this construction method can be subjected to large uplift forces due to heaving

86 soil around the pile. To ensure cracking of the piles does not occur, they can either be

87 adequately reinforced, 'sleeved' (provided with a slip layer) or a combination of these

88   measures can be implemented (Fleming *et al.* 2009). However, in cases where the expansive

89   profile is particularly deep, 'sleeving' and/or socketing into bedrock can become

90   uneconomical. In Kimberley, South Africa, expansive profiles have been found to extend to a

91   depth of up to 30 m (Byrne *et al.* 2019). Other instances of deep expansive profiles have also

92   been reported in Sudan, where it is not uncommon to have expansive profiles extending to

93   greater than 10 m (Elsharie 2012).

94

95   While this foundation type can double the cost of construction (Jennings and Kerrich 1962), if

96   applied correctly, it can result in almost no foundation movements. This foundation type is

97   however, not necessarily a fail-safe approach. Under-prediction of heave can result in the gap

98   between the clay and suspended foundation swelling closed, thereby resulting in uplift of the

99   superstructure.

100

101   A case study where such a design proved to be inadequate was reported by Meintjes (1991).

102   The study reported structural damage due to excessive heave, despite the foundation being

103   designed to have a void of 150 mm between the grade beam and pile cap, and under-

104   reamed/enlarged base piles extending to a depth of 7.7 m.

105

106   Blight (1984) presented the findings of another case study where suspended foundations were

107   used for several buildings at a thermal power plant. While the initial heave calculated for this

108   site was in the order of 120 mm (Blight 1984), this was a gross underestimation of what was

109   observed. Prior to construction, removal of vegetation resulted in rising of the water table,

110   causing far greater heave than what was initially estimated, thereby closing the gap between

111   ground level and the suspended foundation. Some remedial measures implemented at this

112   site have involved increasing the gap between the suspended slabs and the expansive clay

113   to 300 mm. It has been noted that at some buildings at the power plant, these voids have

114   swelled closed yet again (Day 2017).

115

116 This particular case study led to a number of useful investigations on this method of

117 construction. Blight (1984) conducted full-scale pull-out tests on short length piles before and

118 after wetting the profile for a period of 3–4 weeks. His results indicated that an increase in pile

119 pull-out (shaft) capacity was observed after wetting. This finding was in direct contradiction

120 with a study conducted by Elsharief *et al.* (2007) for pile load tests conducted in Sudan. An

121 explanation for this contradiction is that, while the swelling process can produce an increase

122 in lateral stresses against a pile shaft, swell induced softening of the clay (Gens and Alonso,

123 1992) results in a reduction of shear strength which can ultimately reduce shaft capacity. This

124 softening can be viewed as resulting due to a reduction in matric suction, or the structural

125 realignment occurring due to macroscopic volumetric change (i.e. swell) (Gens and Alonso

126 1992). If an engineer is to produce a conservative design for such foundation types, an

127 understanding of these counteracting mechanisms is crucial.

128

129 In an effort to investigate the effects of these mechanisms, Smit *et al.* (2019) presented the

130 results of centrifuge pile pull-out tests. The study involved pull-out tests of bored piles installed

131 in an expansive profile at:

132

133   a) the clay's in-situ water content and

134   b) after allowing swell to occur.

135

136 The results of this study indicated that, after achieving a targeted magnitude of swell, the pull-

137 out capacity of piles reduced by between 57 and 67% when compared to their capacities at

138 the clay's in-situ water content.

139

140 While the results of this preliminary study indicate average shaft friction along the full length

141 of the pile, they give no information on the variation in shaft (pull-out) capacity with depth.

142 Furthermore, such tests investigate the consequence of the two counteracting mechanisms

143 (softening and changes in lateral stresses) without measuring these quantities directly. This

144   study presents a series of centrifuge models aimed to address these shortcomings and

145   provide insights into the aforementioned counteracting mechanisms.

146

147   The first three tests presented in this study involve pull-out tests conducted on short length

148   piles (plugs) at various depths throughout the clay profile. The intention of these tests is to

149   investigate the effect of confinement on the evolution of pile shaft capacity before and after

150   swell. The final test incorporates the use of an aluminium pile, instrumented to measure the

151   change of lateral pressures on the pile shaft throughout the swelling process. This

152   instrumented pile test also included in-flight penetration tests at the clay's in-situ moisture

153   content and after allowing swell to occur. The purpose of this strength characterisation was to

154   obtain an indication of the magnitude of swell-induced softening.

155

156   ***Basic soil classification***

157   The material tested in this study was a highly expansive clay, sampled from the Limpopo

158   province of South Africa, 350 km northeast of Pretoria. The material was sampled from the

159   upper 1.5 m of the profile and can be described as a stiff, fissured and slickensided black clay

160   containing fine nodular calcrete (Day 2020).

161

162   Basic classification tests were performed to establish the soil's particle size distribution (by

163   method of sieving (ASTM 2017a) and hydrometer (ASTM 2017b)), Atterberg limits (ASTM

164   2017c) and specific gravity (ASTM 2014a). These results, as well as the unified soil

165   classification (ASTM 2017d) are presented in Fig. 1 and Table 1. X-ray diffraction testing to

166   determine the mineralogical composition of the clay was performed on the same site by a

167   previous researcher, the results of which are shown in

168   Table 2

169
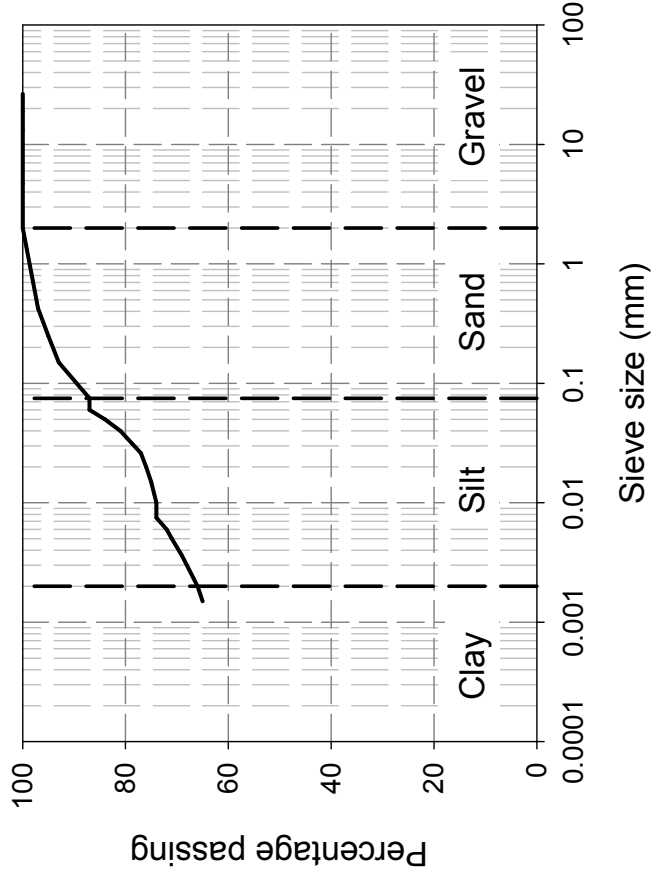
Fig. 1. Particle size distribution

Table 1. Soil classification data

Liquid limit (%)	92
Plasticity index	55
Linear shrinkage (%)	25.5
Activity	0.8
Specific gravity	2.65
Unified soil classification	CH

170
171
172
173
174
175
176
177
178
179
180
181

182   **Table 2. Mineralogical composition based on X-ray diffraction (after Moses 2008)**

Mineral	Composition (%)
Smectite	58
Palygorskite	19
Calcite	5
Plagioclase	5
Quartz	4
Enstatite	4
Kaolinite	3
Diopside	2

183

184   ***Characterisation of swell properties***

185   The mechanical properties of both compacted and undisturbed samples of the clay considered

186   in this study was presented by Gaspar *et al.* (2022). The following section presents a summary

187   of the oedometer tests conducted to quantify the swell properties of the tested clay. For the

188   swell tests, data is presented for both compacted and undisturbed specimens (prepared from

189   block samples). In doing so, the extent to which the laboratory prepared specimens replicated

190   the undisturbed swell behaviour could be assessed.

191

192   Recognising the difficulties associated with preserving the fissured macrofabric of expansive

193   clays during the sampling process, the preparation procedure implemented was aimed

194   towards introducing a certain degree of 'fissuring' for samples prepared in the laboratory. This

195   was accomplished by breaking down intact lumps of clay with a cheese grater at their in-situ

196   water content (approximately 31%) and statically compacting the broken-down clay to a

197   targeted dry density of 1350 kg/m^3. These initial conditions were selected as they are

198   representative of the measured in-situ properties of the clay after the dry season. The rationale

199   for targeting properties related to this season is that they present the most critical case if swell

200   properties are to be measured (i.e. assessing the soil in its driest practical state allows for the

201   largest estimates of swell magnitude and swell pressure to be obtained).

202

203   This preparation procedure differs slightly from more conventional approaches whereby air-

204   dried soil is mixed with a predetermined quantity of water, allowed to equilibrate, and

205   compacted to a target dry density (Monroy *et al.* 2015; Manca *et al.* 2016). The drawback of

206   this more conventional approach, however, is that it results in a fabric with macropores which

207   are relatively isolated. This is in contrast to the fabric type more commonly associated with

208   expansive clays which consists of a series of interconnected pores (i.e. fissures) that more

209   easily facilitate the ingress of water.

210

211   To investigate the swell properties of the compacted and undisturbed specimens, a series of

212   *wetting after loading tests* (ASTM 2014b), sometimes referred to as *swell under load* tests,

213   were conducted at various applied stresses. Such tests involve placing an unsaturated sample

214   into the oedometer, applying a predetermined stress (referred to as the soaking stress) and

215   then flooding the housing with distilled water. As the sample is inundated, volumetric changes

216   are monitored until such point that these changes become negligible. Once volumetric

217   changes cease, the sample is considered as having reached a state of zero suction (Schreiner

218   1988) and the final volumetric strain is noted for that stress level. Table 3 presents the initial

219   sample properties for the oedometer swell tests. Fig. 2 illustrates the results of wetting after

220   loading tests for both the compacted and undisturbed specimens conducted at several values

221   of applied vertical stress. Linear regression curves have also been superimposed onto the

222   dataset for both the compacted and undisturbed samples.

223

224

225

226

227

228　**Table 3. Initial sample properties for oedometer swell tests**

| Description	Soaking stress (kPa)	Void ratio, e	Gravimetric water content, w (%)	Degree of saturation, S_r (%)	Dry density (kg/m³)
Compacted	12.5	0.969	33.6	91.9	1346
Compacted	25	0.971	33.6	91.6	1344
Compacted	50	0.908	30.3	88.5	1389
Compacted	100	0.938	32.2	90.9	1367
Compacted	200	0.973	34.6	94.4	1343
Compacted	300	1.037	34.6	88.6	1301
Compacted	400	1.027	34.6	89.4	1307
Undisturbed	12.5	0.939	31.5	89.0	1367
Undisturbed	25	0.888	30.3	90.5	1403
Undisturbed	50	0.817	29.5	95.6	1459
Undisturbed	100	0.889	30.2	90.2	1403
Undisturbed	200	0.901	29.9	87.8	1394
Undisturbed	300	0.992	30.3	81.0	1331
Undisturbed	400	1.020	32.0	83.2	1312
Undisturbed	500	1.068	30.8	76.3	1281

229

230

231
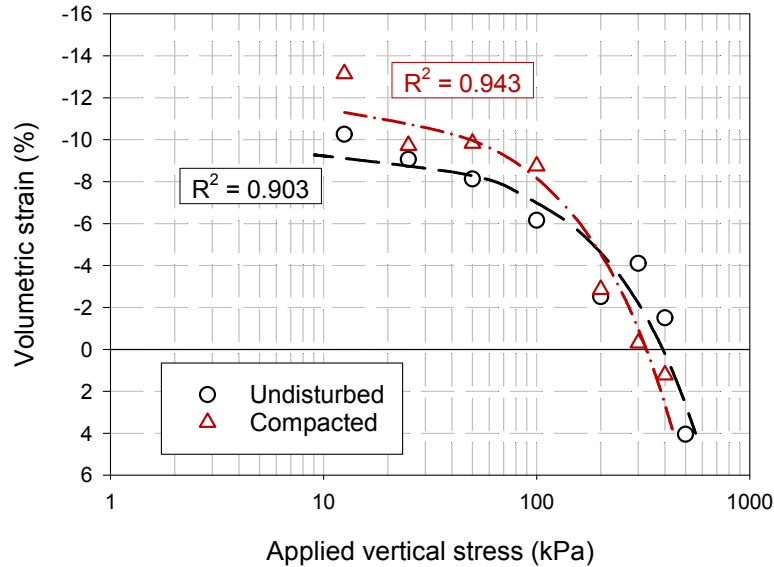
232   **Fig. 2. Soaking under load curves for compacted and undisturbed samples**

233

234   From Fig. 2 it can be seen that the measured swell properties of the compacted and

235   undisturbed specimens are similar. Not only was the magnitude of swell achieved at all

236   soaking stresses similar for the compacted and undisturbed samples, but the swell pressure

237   also remained close. Using the regression curves plotted in Fig. 2, the stress required to

238   achieve 0% volumetric change was 329 and 392 kPa for the compacted and undisturbed

239   specimens respectively. Such results illustrate that the sample preparation procedure

240   implemented was able to retain key swell characteristics of the undisturbed material. In light

241   of this finding, the same approach was implemented in the preparation of the centrifuge

242   models presented in the following section. It should also be highlighted that Gaspar et al.

243   (2023) also reported the saturated hydraulic conductivity (k_{sat}) to be in the range of 10^{-9}-10^{-12}

244   m/s. These values were obtained by applying consolidation theory ($k_{sat} = c_v.m_v.\gamma_w$) to calculate

245   k_{sat} from a consolidation test on a sample reconstituted at 1.1 times the soil's liquid limit.

246

247   ***Model descriptions***

248   This section provides details of the centrifuge tests conducted in this study. First, a description

249   of the clay profile and its preparation is provided. Additionally, aspects of the model layout

250　which are common to all tests are outlined. Thereafter, specific reference is made to the

251　position of piles within the clay profile, as well as the sequence that was followed for each

252　individual test. Unless otherwise stated, all dimensions provided in figures are in model scale.

253　Full-scale (prototype) lengths can be obtained by multiplying model dimensions by the model

254　scaling factor (N=30).

255

256　The centrifuge tests described in this study modelled an expansive soil profile comprising of a

257　stack of 5 clay layers (50 mm thick), statically compacted to a targeted dry density and

258　gravimetric water content of 1350 kg/m^3 and 31% respectively (the average in-situ values

259　determined from site investigations). It should be noted that at this state, the clay layers had

260　a matric suction of approximately 2 MPa. The clay layers were separated by needle punched,

261　non-woven geotextiles. The inclusion of geotextiles in the centrifuge models presented is to

262　facilitate the rapid ingress of water. Additionally, the geotextiles were sized such that hydraulic

263　contact could be maintained between geotextiles separating the clay layers, and the adjacent

264　water wells (described at the end of this paragraph). By controlling the length of the respective

265　geotextiles, an effort was made to avoid any anchorage of the geotextiles at their ends such

266　that they were able to move freely in the vertical direction as swell occurred, and not provide

267　stiffness to the profile. The five clay layers were laterally restrained in position by two

268　perforated steel plates, covered with the same geotextile used to separate the clay layers. The

269　two spaces on either side of the model were used as water wells to facilitate the ingress of

270　water. All tests presented in this study were performed at a centrifugal acceleration of 30 g.

271

272　The layout of the first two tests presented in this study, shown in Fig. 3, were identical and

273　incorporated 4 short-length piles (plugs) installed at various depths. For Test 1, the plugs were

274　pulled out of the profile at the clay's in-situ water content. In this study the "pull-out" capacity

275　is defined as the force required to mobilise peak shaft resistance between the bored piles and

276　surrounding clay. Water was subsequently introduced into the strongbox through inlets at the

277　bottom of the model until the water level was approximately 20 mm above the surface of the

278   top layer. Once the flooding process was complete, every clay layer had access to water on

279   all four boundaries (top, bottom and sides). The front and back of the model were confined

280   between the strongbox's glass window and an aluminium partition plate. After achieving the

281   targeted value of swell, $\approx$ 6.8 mm model scale, (as predicted by the Van der Merwe (1964)

282   empirical prediction method for a clay of *very high potential expansiveness*), the plugs were
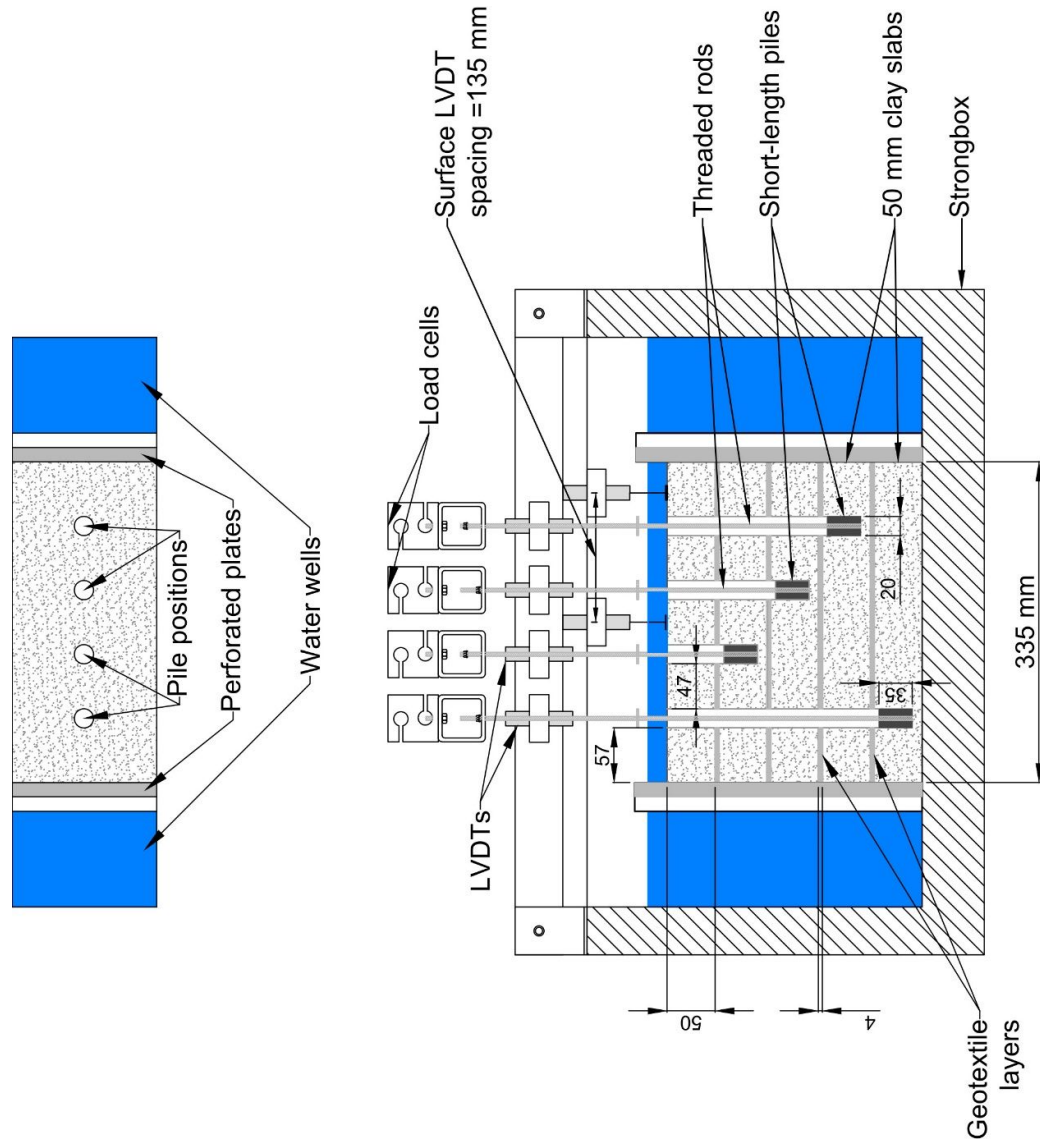
283   pulled for a second time.

284

285   For the second test presented, pull-out tests were only conducted after the targeted swell was

286   achieved. From Fig. 3 it can be seen that the augered holes above the short length piles were

287   unsupported. As a result, clay was able to swell behind the plug as the strongbox was flooded.

288   To investigate the effect of the augered holes swelling closed above the plugs, a final pull-out

289   test was conducted whereby an aluminium tube was used to support the holes during swell

290   (all other aspects of the model layout remaining unchanged). The plugs were then pulled out

291   at the same magnitude of vertical swell as was done for the previous tests. An illustration of

292   the augered hole support is presented in Fig. 4. As shown in Fig. 4, a gap of 5 mm was left

293   between the top of the piles and the aluminium tube. The purpose of this gap was to ensure a

294   that the peak shaft resistance of the piles could be mobilised before making contact with the

295   supporting tube. Furthermore, the tube was clamped at the surface to ensure that this gap

296   was maintained, even as the soil swelled.

297

298   For all three pull-out tests, plugs were cast from a rapid hardening grout with a 4 mm stainless

299   steel threaded rod at their centres. Comparisons of material properties of this grout with a

300   scaled concrete mix developed for centrifuge modelling (Louw *et al.* 2020) indicated that the

301   two materials had similar mechanical properties (Gaspar 2020). Furthermore, the load and

302   displacement of piles throughout testing were monitored using load cells and linear variable

303   differential transformers (LVDTs) respectively in all three tests. It should be noted that for all

304   three pull-out tests, each short-length pile in a given model was pulled out individually (rather

305   than all piles in a model being pulled at the same time). It was therefore possible to ensure

306 that the testing of a single pile did not induce displacements throughout the model which might

307 affect testing of adjacent piles. Additionally, LVDTs were also used to measure swell

308 magnitude at the surface of the clay profile.

309

Fig. 3. Model layout for Tests 1 and 2

310

311

312

Tube clamped into position

Threaded rod

Aluminium tube

5 mm gap

Short pile

313

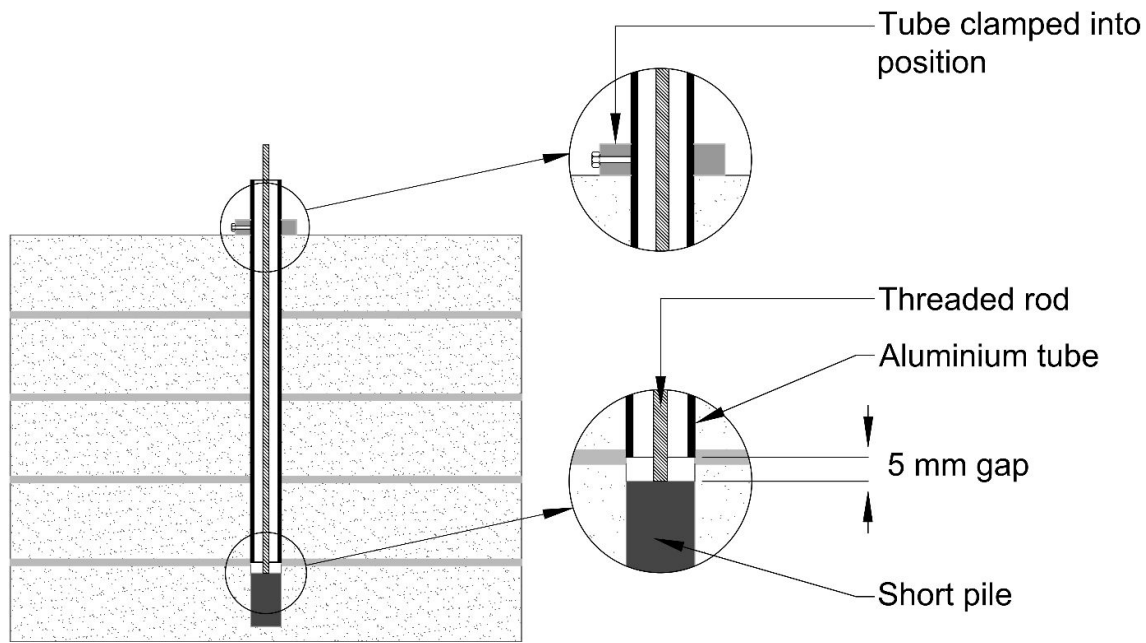314   **Fig. 4. Setup used to support augered holes behind piles**

315

316   The layout of the final test is illustrated in Fig. 5. The test consisted of a single aluminium pile

317   in the centre of the model (anchored at its base), instrumented with lateral load cells positioned

318   at the centre of each clay layer. Measuring 19.05 mm in diameter, the pile was placed in a thin

319   latex membrane (prior to being inserted into the pre-augured hole) to protect instrumentation

320   from the water that would ultimately be introduced into the strongbox. The pile was then

321   inserted (from the top of the profile) into an augered hole with a 20 mm diameter.

322

323   For the instrumented pile, the lateral load cells used were designed, based on an approach

324   suggested by Jacobsz (2002). The load cells were manufactured from aluminium using a

325   process referred to as electrical discharge machining (EDM). As shown in Fig. 6, the load cells

326   comprised of two rounded surfaces and an inner web measuring 0.3 mm in thickness. This

327   web was instrumented on either side with 1 kΩ strain gauges and wired into a full-Wheatstone

328   bridge configuration. Once slotted into the aluminium pile, the rounded edges of the load cells

329   fitted flush with the outer diameter of the pile as illustrated in Fig. 7.

330
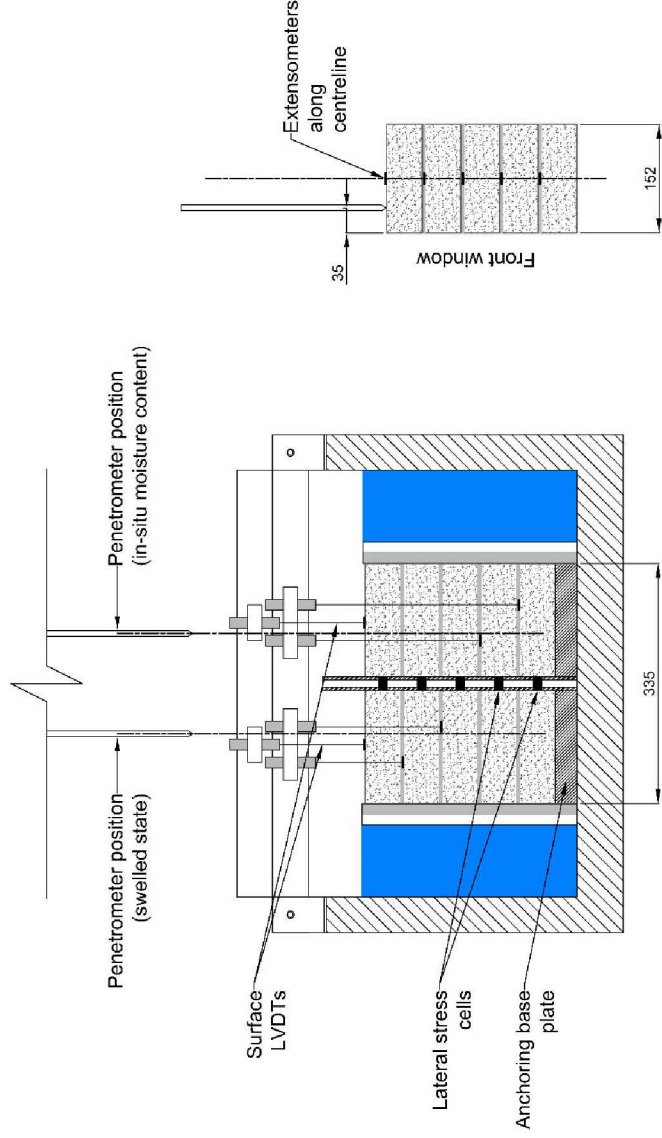
Fig. 5. Instrumented pile test
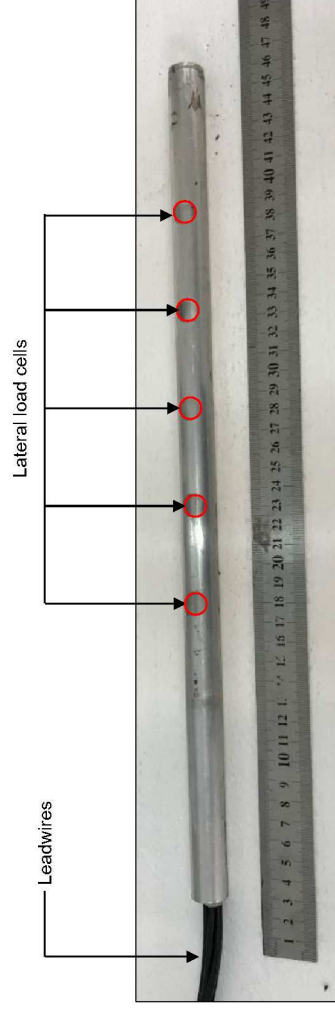
331
332
333

Fig. 6. Un-instrumented lateral load cells

334
335
336

Fig. 7. Assembled instrumented pile

337
338
339

340　This test sequence involved accelerating the model to the desired centrifugal acceleration of

341　30 *g* at the clay's in-situ water content. The strongbox was then flooded with water, inducing

342　swelling of the profile. Throughout the swell process, changes in lateral stresses against the

343　pile shaft were monitored. Additionally, strength measurements of the profile were performed

344　in-flight by means of cone penetration testing (CPT). CPTs were performed at the clay's in-

345　situ water content, and after the targeted swell magnitude had been achieved (that predicted

346　by Van der Merwe (1964) for a clay of *very high potential expansiveness*). The CPT

347　measurements for this test are presented in Fig. 8. Also included in Fig. 8, are CPT

348　measurements conducted in a greenfield centrifuge test (i.e. considering only a soil profile with

349　no external structures or loads) conducted on the same soil type for the same model layout

350　(Gaspar *et al.* 2023).

351

352　While holes were cut in the geotextiles to provide a path for the penetrometer to pass through,

353　the penetrometer punched through the bottom two geotextile layers during the instrumented

354　pile test, as indicated in Fig. 8. In Fig. 8 the prefixes "GF" and "IP" in the legend indicate the

355　greenfield and instrumented pile tests respectively.

356

357　From this figure, it can be seen that the penetration resistance reduced substantially during

358　the swell process. Furthermore, CPTs performed at the clay's in-situ water content and after

359　achieving the targeted swell are similar for the instrumented pile test and the greenfield test.

360　This finding provides confidence that the sample preparation procedure implemented for these

361　two tests, as well as for the pull-out tests discussed previously, produced specimens with

362　consistent strength. Similarly, it illustrates that any tests performed after achieving the targeted

363　swell were also carried out under comparable conditions. Key details of the four centrifuge

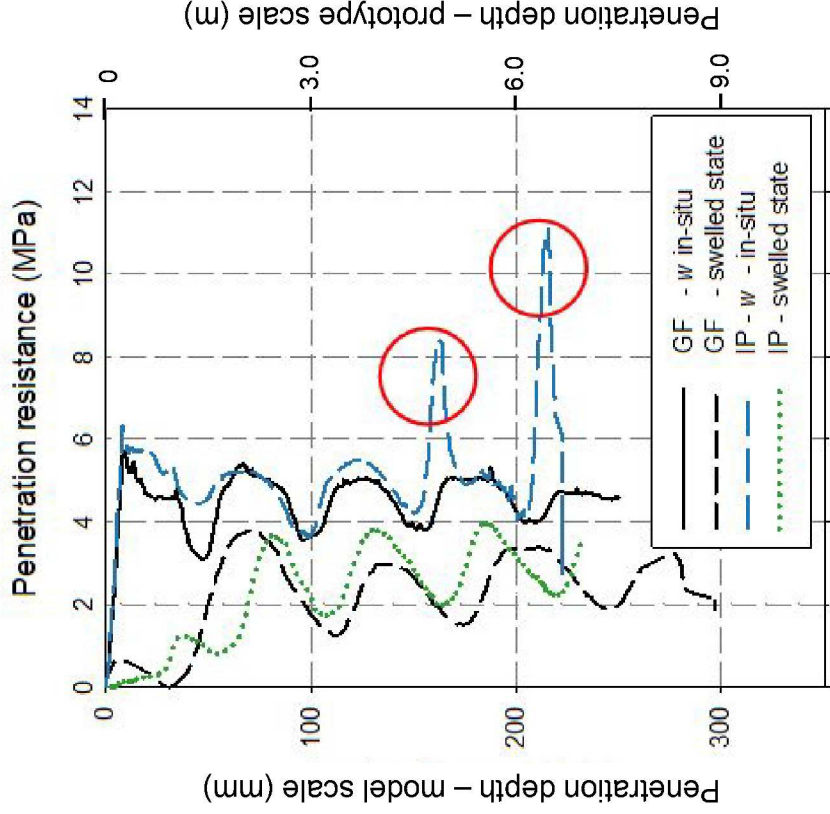364　tests conducted are highlighted in Table 4.

365

366

Fig. 8. Penetration results for the greenfield (GF) (after Gaspar *et al.* (2023)) and instrumented pile (IP) tests

367
368
369
370
371
372
373
374
375
376
377
378
379
380
381

382   **Table 4: Test program**

| Test ID	Pile material	Pile dimensions (model) – length (L); diameter (D) (mm)	Pile dimensions (prototype) – length (L); diameter (D) (m)	Testing period
T1	Rapid hardening grout	L = 35 D = 20	L = 1.05 D = 0.6	Before and after swell
T2	Rapid hardening grout	L = 35 D = 20	L = 1.05 D = 0.6	After swell
T3_S	Rapid hardening grout with aluminium tube supporting holes	L = 35 D = 20	L = 1.05 D = 0.6	After swell
T4_I	Aluminium (instrumented)	L = 355 D = 19	L = 10.65 D = 0.57	From in-situ water content, throughout swell process

383

384   ***Results***

385   The results presented by Smit *et al.* (2019) revealed that the pull-out (shaft) capacity of full-

386   length piles reduced after allowing swell to occur. The aim of the plug pull-out tests was to

387   investigate the dependency of plug pull-out capacity on confinement (overburden) stress at

388   various depths.

389

390 ***Plug pull-out capacity (Test 1)***
391 This series of pull-out tests aimed to investigate the pull-out capacity of piles prior to swell, i.e.

392 at the soil's in-situ water content. After obtaining the pull-out capacity of the plugs at their in-

393 situ water content, the model was flooded to allow the targeted swell to be achieved. Once

394 reached, the plugs were pulled a second time. Fig. 9 illustrates the mobilised shaft friction

395 versus plug displacement during the pull-out tests, prior to and after swell.

396

397   (a)   (b)
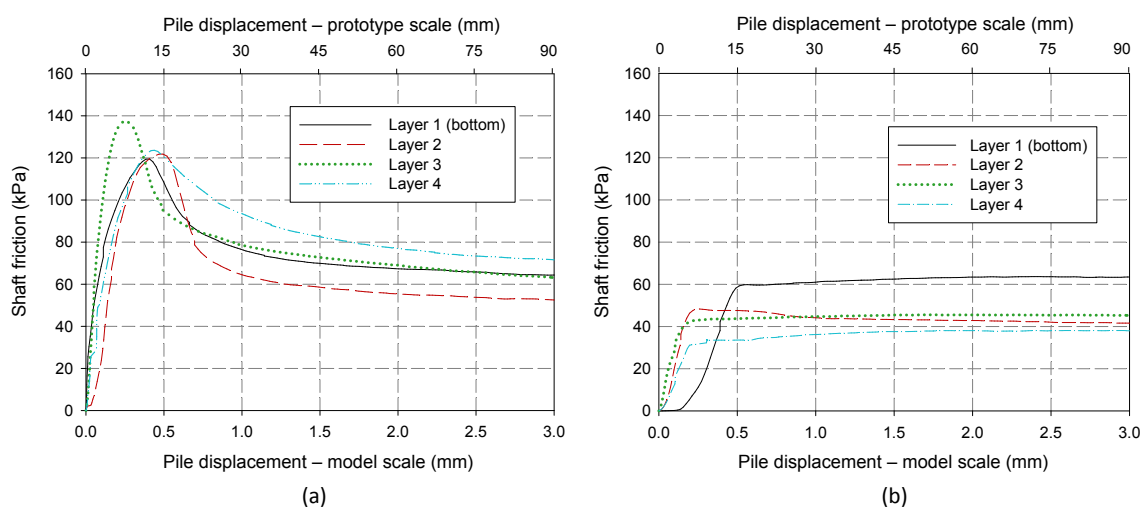
398 **Fig. 9. Mobilised shaft friction versus pile displacement at a) the soils in-situ moisture content and b) after swell had**
399 **occurred during pull-out tests**

400

401 From Fig. 9a) it can be seen that peak shaft friction was achieved at approximately 0.4 mm

402 (0.02 pile diameter) displacement for all plugs except that in Layer 3, which reached its peak

403 at approximately 0.25 mm (0.0125 pile diameter). Fig. 9a) illustrates that the peak shaft friction

404 achieved appears independent of depth within the model and thus of confining pressure. Three

405 of the piles consistently reached a peak shaft friction of approximately 120 kPa, with the plug

406 in Layer 3 achieving a peak shaft friction of close to 140 kPa.

407

408 Fig. 9b) presents the pull-out results for the same plugs after the targeted swell had been

409 reached. In this figure, no peak is observed, but rather all piles appear to reach a certain value

410 of shaft friction and then remain constant. Since this figure presents the results of piles which

411 were previously pulled out of the soil, it might be expected that the maximum shaft friction

412 attained with any further "pulling" would be equivalent to the residual value observed in Fig.

413 9a). This argument is supported by considering that a failure plane would already have been

414 established during the first pull-out test. However, upon closer inspection, it can be seen that

415 there are some differences between the maximum values of shaft friction attained in Fig. 9b)

416 and the values of residual friction observed in Fig. 9a). These differences can be attributed to

417 the softening that occurred during the swell process.

418

419 The largest difference is for the plug in the surface layer (Layer 4) where the lowest confining

420 stress of the 4 plugs would have been experienced. The smallest difference was for the plug

421 in Layer 1 at the bottom of the model (experiencing the highest confining stress). The result in

422 Fig. 9 can be interpreted within the extended Barcelona Basic Model for Expansive Clays

423 (BExM). For this interpretation, it is useful to consider Fig. 10 which highlights the stress state

424 at various positions in the profile in relation to the load collapse (LC) yield curve. In this figure,

425 all 4 layers begin at the same value of suction (s_i). The macroscopic expansion associated

426 with the reduction in suction results in soil softening, which can be represented as the

427 movement of the LC yield curve to the left. The extent of this movement is related to the

428 position of the initial stress state relative to the LC curve. For lower net-mean stresses, the

429 initial stress state is further from the LC curve and will therefore result in the most softening.

430

431 It should be noted that in Fig. 10, it has been assumed that the suction within the bottom 4

432 clay layers reduced by approximately the same amount. This is supported by the consistent

433 CPT measurements for these layers as presented in Fig. 8. As overburden stress increases

434 with depth, swell is incrementally restricted to a larger degree. For this reason, the magnitude

435 of swell-induced softening becomes negligible in the bottom layer, where very little swell

436 occurred. Conversely, in the top layer where the most swell was observed, the effects of swell-

437 induced softening produced the differences between the residual shaft friction in Fig. 9a) and

438 the peak shaft friction in Fig. 9b).

439

440
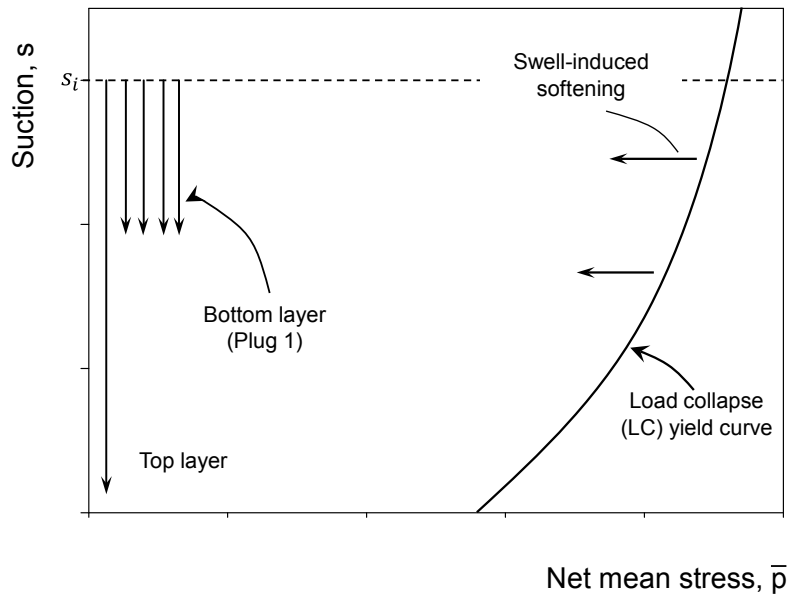
Fig. 10. Interpretation using the BExM framework

442

Plug pull-out (Test 2-after swell)

The model layout for Test 2 was identical to that presented in the previous section. However, for this test, plugs were only pulled once the targeted swell magnitude had been achieved, as opposed to pull-out at the in-situ moisture content in the previous test. Fig. 11 illustrates the results of this pull-out test.

448
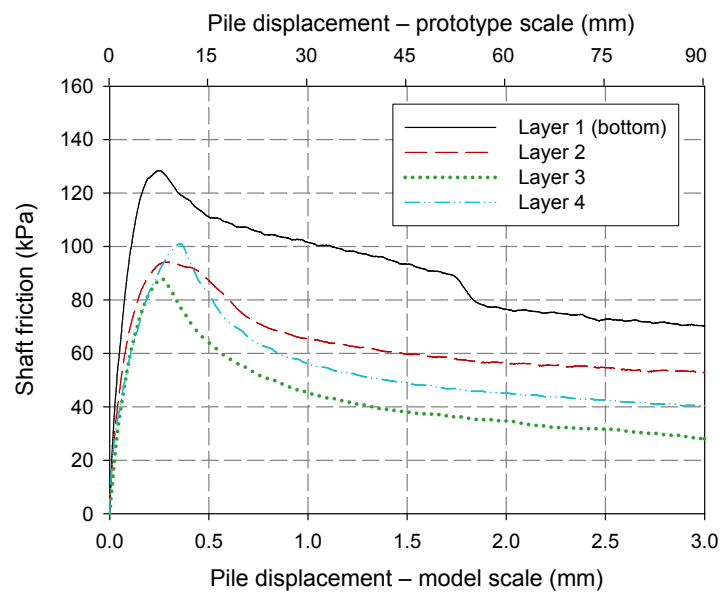
Fig. 11. Pull-out test after swell (unsupported holes)

451

452   In the study conducted on full-length piles by Smit *et al.* (2019), it was found that the pull-out

453   (shaft) capacity reduced by approximately 60% following swelling. Similarly, the results

454   presented in Fig. 11 show a reduction in shaft resistance for all layers, except Layer 1 (at the

455   bottom of the model). In describing the possible mechanisms responsible for the observed

456   increase in pull-out capacity after swell, Blight (1984) attributed his finding to an increase in

457   lateral pressure against the piles. Conversely, Elsharief (2007) attributed the observed

458   reduction in shaft resistance after wetting, to post-swell softening.

459

460   The results of the centrifuge models presented thus far illustrate that there is a relationship

461   between overburden stress and the dominant mechanism governing pile shaft capacity after

462   swell. Closer to the surface, swell is allowed to occur more freely, and so swell-induced

463   softening is the dominant mechanism. At depth where swell is restricted by overburden stress,

464   so too is swell-induced softening and, as such, shaft capacity remains relatively unchanged

465   during and after the wetting process.

466

467   Fig. 12 illustrates a typical example of a plug just after being removed from the model. From

468   this photo, it is evident that during a pull-out test, failure occurs within the clay rather than

469   along the pile/soil interface as may be expected for a perfectly smooth (e.g. aluminium) pile.

470   This observation is in agreement with what was observed by Smit *et al.* (2019).

471

472
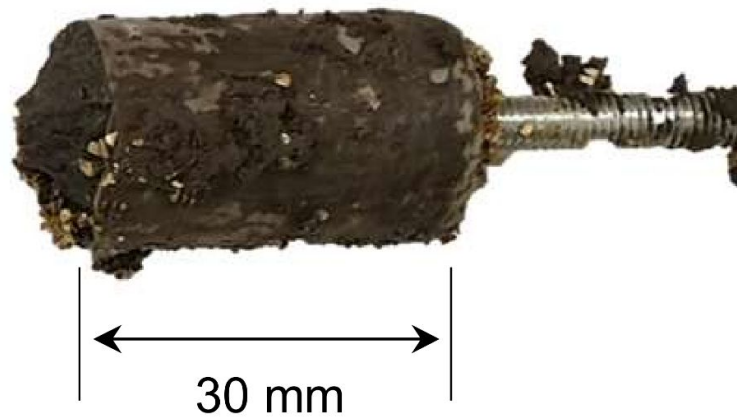
473

474 **Fig. 12. Photograph of short length pile after being pulled out of a swelled profile**

475

476 ***Plug pull-out (Test 3 – after swell - supported holes)***
477 The final pull-out test had the same layout as the previous two tests, except for the fact that

478 the holes above the plugs were supported with aluminium tubes. This test was performed to

479 determine to what degree (if any) the clay which swelled above the plugs affected the

480 measured pull-out (shaft) capacities. Fig. 13 presents the results of the two pull-out tests

481 conducted after swell with and without supported holes.

482

483 (a)   (b)
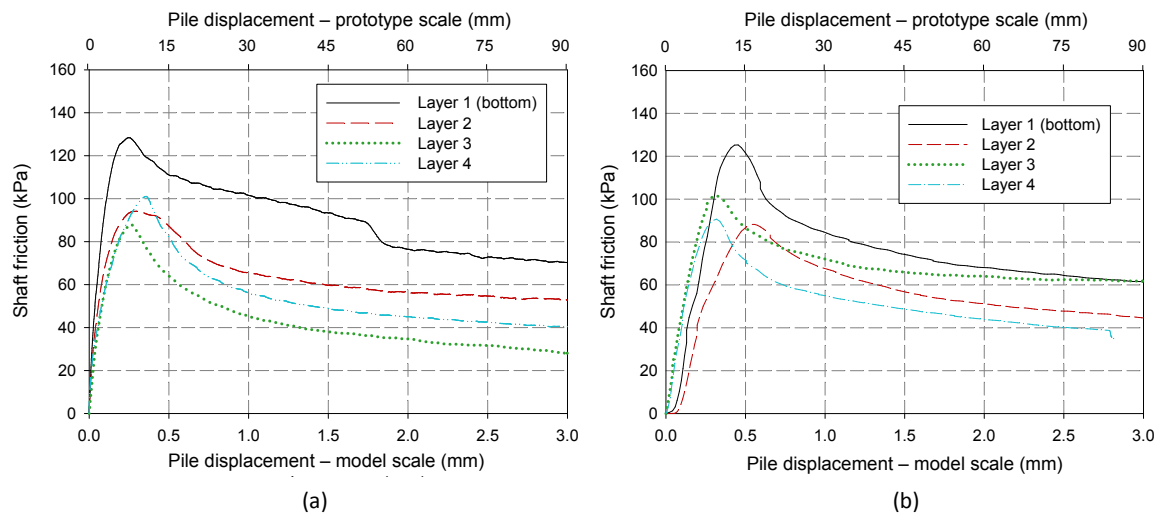
484 **Fig. 13. Plug pull-out tests conducted after achieving the targeted swell for a) unsupported holes and b) supported holes**

485

486 The result presented in Fig. 13 illustrates that the soil swelling above the plugs for the test with

487 unsupported holes had a negligible effect on the measured peak shaft friction. This can be

488   attributed to the fact that the soil which was allowed to swell behind the plug had softened

489   significantly.

490

491   Fig. 14 presents the results of peak shaft friction (i.e. pull-out capacity) for the various pull-out

492   tests conducted. On the primary vertical axis (left) the overburden stress has been calculated

493   from the initial unit weight of the various layers. The secondary vertical axis (right) illustrates

494   the position of the plug as the height above the base of the model in model scale. A third

495   vertical axis (far right) presents the height above the base of the model in prototype scale. The

496   results of the pull-out tests have also been summarised in Table 5.

497

498

499   **Fig. 14. Comparison of pull-out capacities for the various pull-out tests conducted**
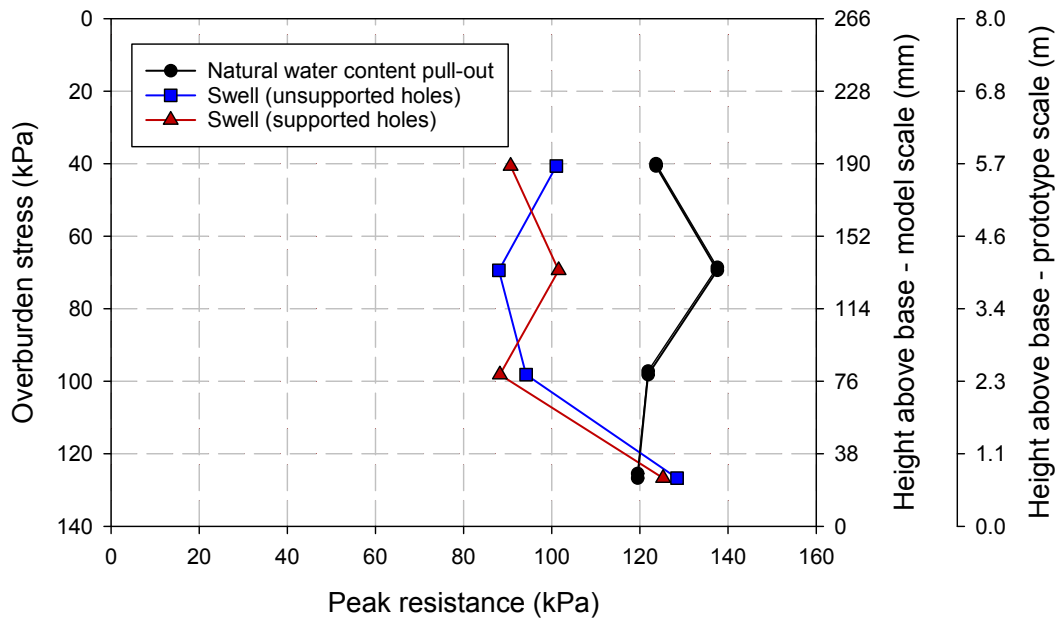
500

501

502

503

504

505

506

507 **Table 5: Summary of pull-out test results**

| Test ID	Layer	Peak friction – before swell (kPa)	Residual friction – before swell (kPa)	Peak friction – after swell (kPa)	Residual friction – after swell (kPa)
T1	1	119.5	64.4	63.5	NA
	2	121.8	72.0	41.6	NA
	3	137.6	63.1	45.2	NA
	4	123.6	52.5	37.9	NA
T2	1	NA	NA	128.3	69.0
	2	NA	NA	94.3	52.7
	3	NA	NA	87.8	27.6
	4	NA	NA	101.0	39.9
T3_S	1	NA	NA	125.3	61.0
	2	NA	NA	88.2	44.3
	3	NA	NA	101.6	61.6
	4	NA	NA	90.7	38.8

508

509   The results in Fig. 14 illustrate that in general, there is a reduction in pull-out capacity of piles

510   after allowing swell to occur. However, at high confining/overburden stresses, pull-out capacity

511   appears to be unchanged (and may increase locally) since the restriction of vertical swell

512   results in a reduction of swell-induced softening. Fig. 14 also illustrates good repeatability in

513   test results for piles pulled out after achieving targeted swell.

514

515   ***Instrumented pile test***

516   The purpose of this test was to measure changes in lateral swell pressure against the pile

517   shaft throughout the swell process. It should be highlighted that after installation, there was a

518   gap estimated at approximately 0.5 mm between the augered hole perimeter and the pile. As

519   a result, some expansion of the clay would have had to occur before contact was made with

520   the pile. This is an important factor to recognise since any amount of heave can significantly

521   reduce the magnitude of lateral swell-pressure against a structure (Fourie, 1991). For this

522   reason, this test aimed to provide a qualitative illustration of the variation in swell pressure

523   against the instrumented pile. The results of this test are provided in Fig. 15.

524
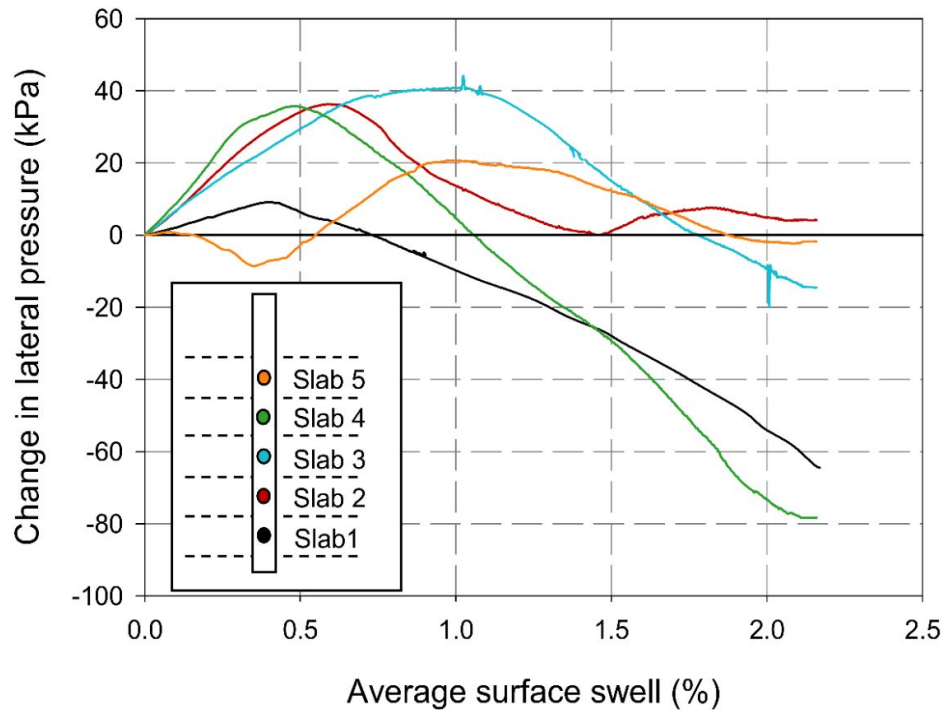
525

526   **Fig. 15. Change in lateral pressure due to swell**

527

528   The results presented in Fig. 15 illustrate the *change* in lateral swell pressure against the pile.

529   Data in this figure was zeroed after the model had been flooded. The data presented extends

530   from the instant that the water level within the strongbox had cleared the top of the surface of

531   the profile to the point at which the targeted swell had been achieved.

532

533   From Fig. 15 it can be seen that the top layer initially experienced a slight reduction in lateral

534   pressure, followed by an increase to approximately 20 kPa. The initial drop in pressure or 'lag'

535   before observing a pressure increase can be attributed to the fact that the aluminium pile was

536   pushed into the augered hole from the top of the profile. Doing so resulted in slight disturbance

537   of the adjacent soil, thereby creating a larger gap between the augered holes and the pile in

538   the top layer. However, the general trend observed for all load cells is that an increase in

539   lateral pressure occurs relatively early in the test, followed by a drop in pressure. This agrees

540   with the results of Schreiner and Burland (1991) of an oedometer test with lateral stress

541   measurement. It also supports the findings of Robertson and Wagener (1975) who observed

542   that the maximum swell induced lateral pressure against abutment walls occurred before

543   complete wetting was achieved.

544

545   The above finding also provides insights into the discrepancies in the publications of Blight

546   (1984) and Elsharief (2007) mentioned earlier. While Blight (1984) and Elsharief (2007)

547   reported an increase and reduction in shaft capacity respectively after wetting of the profile,

548   neither author stated the magnitude of swell that had occurred at the time of testing. A closer

549   investigation of these studies reveals wetting periods of 3-4 weeks (Blight 1984) and 2 months

550   (Elsharief 2007). Considering the results in Fig. 15, it is likely that the tests conducted by Blight

551   (1984) were conducted early in the swell process where there was still an increase in lateral

552   swell pressure against the pile. Similarly, the significantly longer wetting period of Elsharief

553   (2007) place the test in the later stages of the swelling process where swell induced softening

554   becomes the dominant mechanism.

555

556   It is therefore crucial that any tests which aim to investigate the shaft capacity of a pile after

557   swell has occurred, should be considered together with the anticipated magnitude of swell. By

558   not considering the magnitude of anticipated swell, it cannot be stated whether softening or

559   increases in lateral pressure will dominate the behaviour of the pile.

560

561   Even though the results presented in Fig. 15 are meant to provide qualitative illustrations of

562   the variation in lateral stress, the result does at first, appear contradictory to the results of the

563   plug pull-out tests presented previously. The end of the instrumented pile test represents the

564   level of swell at which plugs were pulled out of the profile for the previous tests. Whereas the

565   result presented in Fig. 14 illustrates a relatively unchanged value of pull-out capacity for the

566   bottom plug after swell when compared to the in-situ water content pull-out test, Fig. 15

567   illustrates a reduction in lateral stress in this clay layer. To reconcile these two results, it is

568   important to consider the absolute values of stress throughout the model. The initial

569   overburden stress at the bottom of the top layer and the bottom of the model is approximately

570   27 and 130 kPa respectively. As such, a unit reduction in lateral pressure at the latter stages

571   of a swell process will have a much more significant impact on the shaft capacity in upper

572   portions of the profile.

573

574   ***Conclusions***

575   The results of the centrifuge tests presented in this study illustrate that the shaft (pull-out)

576   capacity of a pile after allowing swell to occur is dependent on both overburden stress (depth

577   in the profile) and on the magnitude of swell which has occurred. At the clay's in-situ water

578   content, pull-out tests revealed no dependency of shaft capacity on overburden stress.

579   However, after achieving a targeted value of swell (that predicted by Van der Merwe (1964)

580   for a clay of very high potential expansiveness), a reduction in pull-out capacity was observed

581   in the upper portions of the clay profile. This reduction in capacity can be attributed to swell-

582   induced softening of the surrounding clay. Conversely, for short-length piles (plugs) tested at

583   higher confining stresses, pull-out capacity remained relatively unchanged when compared to

584   that measured under in-situ moisture conditions. An explanation for this finding is that at depth,

585   where swell is largely restricted, so too are the effects of swell-induced softening.

586

587   In addition to the dependency on overburden stress, it was found that the change in lateral

588   stresses against a pile is strongly dependent on the magnitude of heave which has occurred.

589   Regardless of the position within a profile, lateral stresses tend to increase in the early stages

590   of a swelling process and then reduce as heave continues. The lowest value of shaft

591   resistance throughout the lifetime of a structure may either be at the clay's in-situ moisture

592 content, or after a significant magnitude of heave has occurred. If site tests are conducted to

593 determine the shaft resistance of piles in expansive clays, an estimate of the likely magnitude

594 of heave and its variation with depth during the lifetime of the structure is required to achieve

595 a conservative design.

596

607

608 **Competing interests:** The authors declare there are no competing interests.

609 **Authors contribution statement:**

610 Tiago Gaspar: Conceptualization; Methodology; Formal analysis; Investigation; Writing –

611 Original Draft; Visualization

612 Schalk Jacobsz: Conceptualization; Supervision; Funding acquisition; Writing – Review and

613 Editing; Project administration

614 Gerrit Smit: Conceptualization; Methodology; Writing – Review and Editing

615 Ashraf Osman: Conceptualization; Funding acquisition; Writing – Review and Editing; Project

616 administration

617

620   for a project entitled 'Developing Performance based design for foundations of wind turbines

621   in Africa (WindAfrica)', Grant Ref: EP/P029434/1. The first author would also like to

622   acknowledge the Newton Fund UnsatPractice PhD exchange programme (grant Ref:

623   ES/N013905/1), which enabled him to spend six months at Durham University during his PhD

624   study at the University of Pretoria.

625   **Data availability statement:** Data generated or analysed during this study are available from

626   the corresponding author upon reasonable request.

627

628   *References*

629   ASTM (2014*a*). ASTM D854–14: Standard Test Methods for Specific Gravity of Soil Solids by

630   Water Pycnometer, West Conshohocken, P.A.

631

632   ASTM (2014*b*). ASTM D4546–14: Standard Test Method for One-Dimensional Swell or

633   Collapse of Soils, Technical report, West Conshohocken, P. A.

634

635   ASTM (2017*a*). ASTM D6913 / D6913M-17: Standard Test Methods for Particle-Size

636   Distribution (Gradation) of Soils Using Sieve Analysis, West Conshohocken, P.A.

637

638   ASTM (2017*b*). ASTM D7928-17: Standard Test Method for Particle-Size Distribution

639   (Gradation) of Fine-Grained Soils Using the Sedimentation (Hydrometer) Analysis, West

640   Conshohocken, PA.

641

642   ASTM (2017*c*). ASTM D4318-17e1: Standard Test Methods for Liquid Limit, Plastic Limit, and

643   Plasticity Index of Soils, West Conshohocken, P. A.

644

645   ASTM (2017*d*). ASTM D2487-17e1: Standard Practice for Classification of Soils for

646   Engineering Purposes (Unified Soil Classification System), West Conshohocken, P. A.

647

648　Blight, G. E. (1984). Power Station Foundations in Deep Expansive Soil Power Station

649　Foundations in Deep Expansive Soil. *First International Conference on Case Histories in*

650　*Geotechnical Engineering*, Missouri, pp. 77–86.

651

652　Brackley, I. J. A. B. (1975*b*). A model of unsaturated clay structure and its application to swell

653　behaviour. *Proceedings of the 6th African Regional Conference on Soil Mechanics and*

654　*Foundation Engineering*, Vol. 1, pp. 65–70.

655

656　Byrne, G., Chang, N. and Raju, V. (2019). A Guide to Practical Geotechnical Engineering in

657　Africa, 5th Edition edn, FRANKI A KELLER COMPANY.

658

659　Charlie, W. A., Osman, M. A. and Elfatih, M. A. (1985). Construction on expansive soils in

660　Sudan. Journal of Construction Engineering and Management, 110 No. **3**, 359-374

661

662　Day, P. (2017). Challenges and shortcomings in geotechnical engineering practice in the

663　context of a developing country (Terzaghi Oration). *Proceedings of the 19th International*

664　*Conference on Soil Mechanics and Geotechnical Engineering*, Seoul, pp. 11-34.

665

666　Elsharief, A. M., Ahmed, E. O. and Mohamedzein, Y. E. A. (2007). Guidelines for the Design

667　of Bored Concrete Piles in Expansive Soils of Sudan. *Graduate School Conference, on Basic*

668　*Sciences and Engineering*, University of Khartoum.

669

670　Elsharief, A. (2012). Foundations on Expansive Soils, Sudan Experience. *Graduate School*

671　*Conference, on Basic Sciences and Engineering*, University of Khartoum.

672

673　Fleming, K., Weltman, A., Randolph, M. and Elson, K. (2009). Piling Engineering, 3rd edn,

674　Taylor & Francis.

675

676   Fourie, A. B. (1991). Lateral swelling pressure developed in an active clay. *Geotechnics in the*

677   *African Environment*, Maseru, Lesotho, (eds G. E. Blight, A. B. Fourie, I. Luker, D. J. Mouton

678   and R. J. Scheurenberg), Vol. 1, pp. 267–274 Balkema, Rotterdam, Maseru, Lesotho.

679

680   Fredlund, D. G. (1983). Prediction of ground movements in swelling clays. *31st Annual Soil*

681   *Mechanics and Found Engineering Conference*. University of Minnesota, Minneapolis.

682

683   Gaspar, T. A. V., Jacobsz, S. W., Heymann, G., Toll, D. G., Gens, A., and Osman, A. S.

684   (2022). The mechanical properties of a high plasticity expansive clay. *Engineering Geology*,

685   *303*(March), 106647. https://doi.org/10.1016/j.enggeo.2022.106647

686

687   Gaspar, T. A. V., Jacobsz, S. W., Smit, G., Gens, A., Toll, D. G., and Osman, A. S. (2023).

688   Centrifuge modelling of an expansive clay profile using artificial fissuring to accelerate swell.

689   *Engineering Geology*, 312, 106928. https://doi.org/10.1016/j.enggeo.2022.106928

690

691   Gaspar, T.A.V. (2020). *Centrifuge modelling of piled foundations in swelling clays*. PhD

692   Thesis, University of Pretoria, Pretoria, South Africa

693

694   Gens, A. and Alonso, E. E. (1992). A framework for the behaviour of unsaturated expansive

695   clays. *Canadian Geotechnical Journal* **29**, No. 6, 1013–1032.

696

697   Jacobsz, S. W. (2002). The effects of tunnelling on piled foundations, PhD thesis, University

698   of Cambridge September.

699

700   Jennings, J. E. and Kerrich, J. E. (1962). The heaving of buildings and the associated

701   economic consequences with particular reference to the Orange Free State Goldfields. *The*

702   *Civil Engineer in South Africa* **4** No. 11, 221–248.

703

704　Li, J., Cameron, D. and Ren, G. (2014). Case study and back analysis of a residential building

705　damaged by expansive soils. *Computers and Geotechnics*, **56**, 89–99.

706

707　Louw, H., Kearsley, E., and Jacobsz, S. W. (2020). Modelling horizontally loaded reinforced-

708　concrete piles in a geotechnical centrifuge. *International Journal of Physical Modelling in*

709　*Geotechnics* **22** No.1, 14-25

710

711　Manca, D., Ferrari, A., and Laloui, L. (2016). Fabric evolution and the related swelling

712　behaviour of a sand/bentonite mixture upon hydro-chemo-mechanical loadings.

713　*Géotechnique*, *66*(1), pp. 41–57. https://doi.org/10.1680/jgeot.15.P.073

714

715　Monroy, R., Zdravkovic, L., and Ridley, A. M. (2015). Mechanical behaviour of unsaturated

716　expansive clay under K0 conditions. *Engineering Geology*, *197*, pp. 112–131.

717　https://doi.org/10.1016/j.enggeo.2015.08.006

718

719　Moses, A. M. (2008). Mineralogy, Chemistry and Pedological Investigations of the

720　Maandaagshoek 254 kt's Palygorskite deposit: Implication on the Genesis and Industrial

721　Application (Honours report). *University of Pretoria*, Pretoria.

722

723　Meintjes, H. A. C. (1991). A case history on heaving clay: Colinda Primary School.

724　*Geotechnics in the African Environment*, Maseru, Lesotho, (eds G. E. Blight, A. B. Fourie, I.

725　Luker, D. J. Mouton and R. J. Scheurenberg) pp. 99–104.Balkema, Rotterdam.

726

727　Nelson, J. D., Reichler, D. K. and Cumbers, J. M. (2006). Parameters for heave prediction by

728　oedometer tests. *Proceedings of the 4th International Conference on Unsaturated Soils*,

729　Carefree, Arizona, pp. 951–961.

730

731 Pellissier, J. P. (1997). A raft design method for swelling clay. *Proceedings of the 14th*

732 *International Conference on Soil Mechanics and Foundations Engineering*. Hamberg,

733 Germany, pp. 863–869.

734

735 Robertson, A. and Wagener, F. (1975). Lateral swelling pressures in active clay. *Proceedings*

736 *of the 6th African Regional Conference on Soil Mechanics and Foundation Engineering*, vol.

737 1, Durban, pp. 107–114.

738

739 Schreiner, H. D. (1988). *Volume Change of Compacted Highly Plastic African Clays*, PhD

740 thesis, Imperial College London.

741

742 Schreiner, H. D. and Burland, J. B. (1991). A comparison of three swell test procedures.

743 *Geotechnics in the African Environment*, Maseru, Lesotho, (eds G. E. Blight, A. B. Fourie, I.

744 Luker, D. J. Mouton and R. J. Scheurenberg), pp. 259–266, Balkema, Rotterdam

745

746 Smit, G., Gaspar, T. A. V., Jacobsz, S. W. and Osman, A. S. (2019). Centrifuge modelling of

747 pile pull-out tests in expansive soil. *XVII European Conference on Soil Mechanics and*

748 *Geotechnical Engineering*, Reykjavik, Iceland.

749

750 Van der Merwe, D. (1964). The prediction of heave from the plasticity index and percentage

751 clay fraction of soils. *The Civil Engineer* pp. 103–107.

752